MR-Based Targeting of Histotripsy Therapy at 7T

Steven P Allen[1], Timothy L Hall[1], Charles A Cain[1], and Luis Hernandez-Garcia[1]
[1]*Biomedical Engineering, University of Michigan, Ann Arbor, Michigan, United States*

Introduction: In this paper, we investigate the feasibility of using MRI for real-time targeting of ultrasonic cavitation based tissue ablation (histotripsy)[1]. This therapeutic technique uses HIFU induced transient cavitation to liquefy tissue within a small focal volume. The time-dependant behavior of the transient bubble cloud can be described in three stages: 1) rapid expansion over approximately 30 µs, 2) collapse of the cloud over 100 µs, 3) a sparse residual distribution of bubbles lasting up to several hundred ms. We have previously demonstrated [2,3] that the effects of histotripsy on tissue are readily visible by MRI. In contrast, the objective of the present work is to use MRI as a tool for targeting and steering histotripsy therapy in real time.

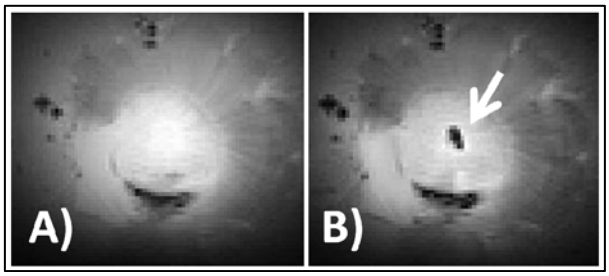

Figure 1: ***GRE acquisition of a coronal slice of lamb kidney (A) without therapy and (B) with therapy. The GRE sequence is sensitive to the cavitation cloud (arrow).***

Methods/Results: Freshly excised lamb kidneys were immersed in saline and secured by sutures in a custom, MR-safe, 7 element transducer, with the elements distributed about a hemisphere. (Aperture/Focal Distance/Frequency/Peak Rarefactional Pressure = 8.5cm/4.5cm/1 Mhz/ >23 MPa).

Coronal slices of the kidneys in the transducer were acquired in a 7T scanner (Varian) using a standard GRE sequence and 1cm radius transmit/receive surface coil. Histotripsy therapy comprised of applying five 3 µs long HIFU pulses, spaced 200 µs apart, immediately after the phase encoding step of the GRE sequence. Images with identical prescriptions were also acquired without the applied histotripsy pulses. Imaging parameters: TR/ TE/ Nex/ FOV/Matrix size/Bandwidth /Flip Angle = 225 ms/6.0 and 7.5 ms /16 /45x45x1mm /128x128x3 /50 kHz /90°. Additionally, B_0 field maps of a single slice both during and after therapy were generated by subtracting the phase of images acquired at 6.0 and 7.5 ms.

The images in Fig. 1 indicate that the GRE sequence is sensitive to the presence of the cavitational cloud (typically ~1mm diameter sphere comprised of ~10 µm diameter bubbles).The magnetic field maps collected before and during treatment are shown in Fig 2 and indicate a perturbation of the magnetic field due to the presence of cavitation.

Discussion: Though the therapeutic bubble cloud exists for only a small fraction of the echo time, Fig 1 shows that it produces a detectable and localized perturbation of the MR signal. Further, we believe that this perturbation originates from three possible sources: 1) enhanced T2* decay due to the susceptibility gradients of the bubbles, 2) motion of the surrounding water during cloud collapse, and 3) the void fraction of the bubbles.

The B_0 field maps in Fig. 2 show that this perturbation behaves similarly to field perturbations caused by the surrounding stationary susceptibility artifacts (formed during the suturing process). This suggests that the majority of the transient cloud's contrast originates from the cloud's own susceptibility gradients.

Future work will focus on implementation using single-shot imaging to minimize the applied treatment dose during the targeting phase of therapy and quantification of the size and distribution of the cavitation bubbles using MR images.

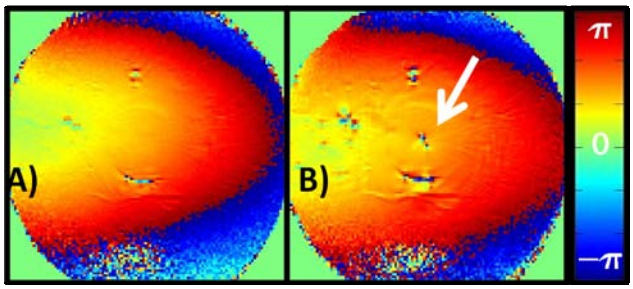

Figure 2: ***Phase subtraction of a single slice (A) without therapy and (B) with therapy. The B_0 field perturbation caused by the therapy cloud (arrow) behaves similarly to the surrounding stationary perturbations formed in the soft tissure during handling. B_0 variation scales linearly with phase. TE = 6.0 and 7.5ms.***

References: 1) Roberts, Hall, J Urol 2006; 175: 734-738. 2) Hall, ISMRM 2007 Berlin; 1118.
3) Allen, et al ISMRM 2012 Melbourne; 1582